



HAL
open science

Cationic Biphotonic Lanthanide Luminescent Bioprobes Based on Functionalized Cross-Bridged Cyclam Macrocyces.

Jonathan Mendy, Anh Thy Bui, Amandine Roux, Jean-Christophe Mulatier, Damien Curton, Alain Duperray, Alexei Grichine, Yannick Guyot, Sophie Brasselet, François Riobé, et al.

► **To cite this version:**

Jonathan Mendy, Anh Thy Bui, Amandine Roux, Jean-Christophe Mulatier, Damien Curton, et al.. Cationic Biphotonic Lanthanide Luminescent Bioprobes Based on Functionalized Cross-Bridged Cyclam Macrocyces.. ChemPhysChem, 2020, 21 (10), pp.1036-1043. 10.1002/cphc.202000085 . hal-02533027

HAL Id: hal-02533027

<https://hal.univ-brest.fr/hal-02533027>

Submitted on 14 May 2020

HAL is a multi-disciplinary open access archive for the deposit and dissemination of scientific research documents, whether they are published or not. The documents may come from teaching and research institutions in France or abroad, or from public or private research centers.

L'archive ouverte pluridisciplinaire **HAL**, est destinée au dépôt et à la diffusion de documents scientifiques de niveau recherche, publiés ou non, émanant des établissements d'enseignement et de recherche français ou étrangers, des laboratoires publics ou privés.

Cationic Biphotonic Lanthanide Luminescent Bioprobes Based on Functionalized Cross-Bridged Cyclam Macrocycles.

Jonathan Mendy,^[a] Anh Thy Bui,^[b] Amandine Roux,^[b] Jean-Christophe Mulatier,^[b] Damien Curton,^[b] Alain Duperray,^[c] Alexei Grichine,^[c] Yannick Guyot,^[d] Sophie Brasselet,^[e] François Riobé,^[b] Chantal Andraud,^[b] Boris Le Guennic,^[f] Véronique Patinec,^[a] Raphael Tripier,^{[a]*} Maryline Beyler^{[a]*} and Olivier Maury^{[b]*}

Abstract: Cationic lanthanide complexes are generally able to spontaneously internalize into living cells. Following our previous works based on diMe-cyclen framework, a second generation of cationic water-soluble lanthanide complexes based on a constrained cross-bridged cyclam macrocycle functionalized with donor- π -conjugated picolinate antennas was prepared with europium(III) and ytterbium(III). Their spectroscopic properties were thoroughly investigated in various solvents and rationalized with the help of DFT calculations. A significant improvement was observed in the case of the Eu^{3+} complex, while the Yb^{3+} analogous conserved photophysical properties in aqueous solvent. Two-photon (2P) microscopy imaging experiments on living T24 human cancer cells confirmed the spontaneous internalization of the probes and images with good signal-to-noise have been obtained in the classical NIR-to-visible configuration with the Eu^{3+} luminescent bioprobe and in the NIR-to-NIR with the Yb^{3+} one.

Introduction

Two-photon lanthanide luminescent bioprobes (2P-LLB) attract more and more attention because they combine in a single molecule the advantages of lanthanide emission (sharp transition ranging from the visible to the near-infrared (NIR) with a large

[a] J. Mendy, Dr. V. Patinec, Pr. R. Tripier, Dr. M. Beyler, Univ Brest, UMR CNRS-UBO 6521 CEMCA, IBSAM, UFR des Sciences et Techniques, 6 Avenue Victor le Gorgeu, C.S. 93837, F-29238, Brest, Cedex 3, France.
E-mail: Maryline.Beyler@univ-brest.fr, raphael.tripier@univ-brest.fr

[b] Dr. A. T. Bui, Dr. A. Roux, J.-C. Mulatier, D. Curton, Dr. F. Riobé, Dr. C. Andraud, Dr. O. Maury, Univ Lyon, ENS de Lyon, CNRS UMR 5182, Université Claude Bernard Lyon 1, F-69342 Lyon, France.
E-mail: olivier.maury@ens-lyon.fr

[c] Dr. A. Duperray, Dr. A. Grichine, INSERM, U1209, Université Grenoble Alpes, IAB, F-38000, Grenoble, France

[d] Dr. Y. Guyot, Univ Lyon, Institut Lumière Matière, UMR 5306 CNRS–Université Claude Bernard Lyon 1, 10 rue Ada Byron, F-69622 Villeurbanne Cedex, France.

[e] Dr. S. Brasselet, Univ Aix Marseille, CNRS, Centrale Marseille, Institut Fresnel, UMR 7249, F-13013 Marseille, France

[f] Dr. B. Le Guennic, Univ Rennes, CNRS, ISCR (Institut des Sciences Chimiques de Rennes), UMR 6226, F-35000 Rennes, France

Supporting information for this article is given via a link at the end of the document.

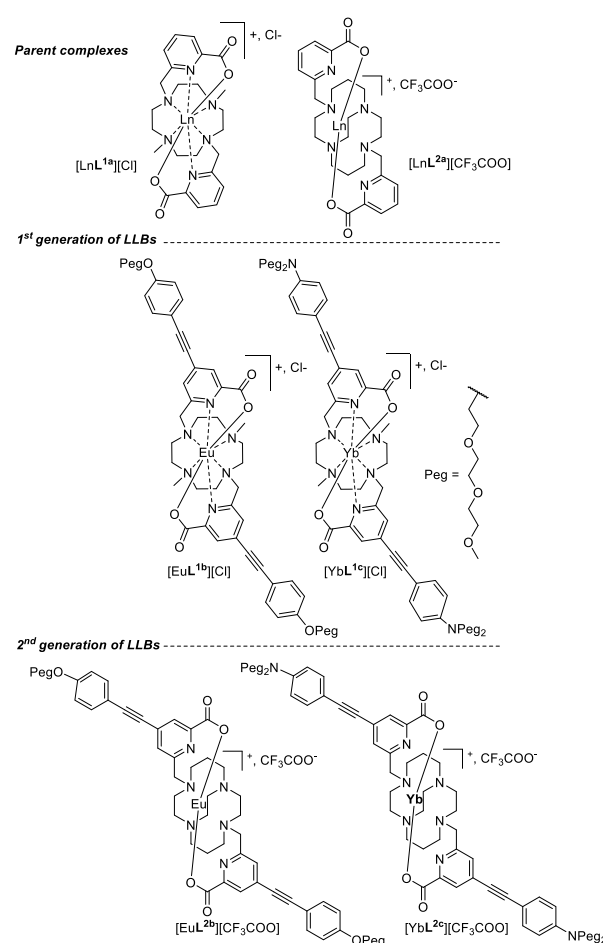


Figure 1. Structure of previously studied lanthanide bioprobes (up) and of a new generation of complexes described in this work (bottom).

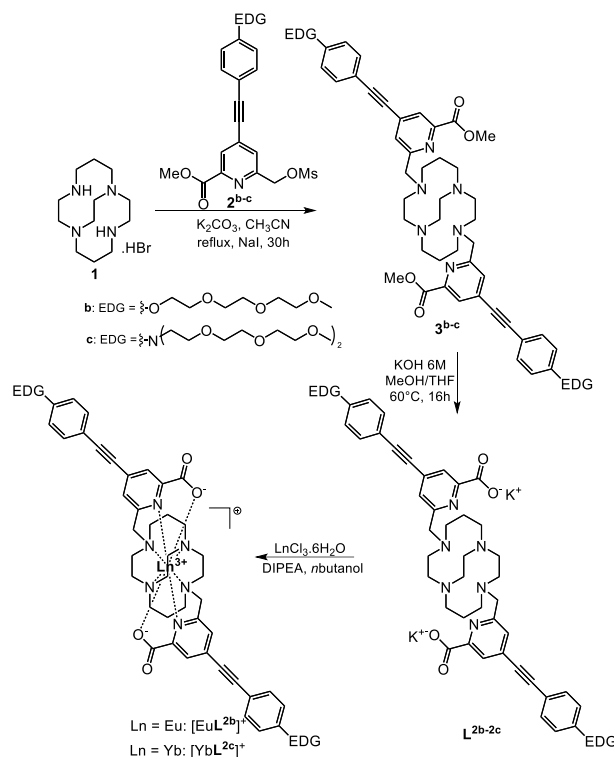
pseudo Stokes shift and a long lifetime from μs to ms , depending on the nature of the central f -emitter) with the intrinsic properties of two-photon excitation (3D resolution, NIR spectral range).^[1] This unique combination of photophysical properties makes these 2P-LLB particularly attractive for bioimaging applications especially when both emission and excitation are localized in the biological transparency window, the so-called NIR-to-NIR microscopy configuration.^[2] This particularly appealing situation can be achieved using ytterbium(III) or to a lesser extend

ARTICLE

samarium(III) 2P-LLB.^[3] The design of such luminescent probes requires to simultaneously fulfil conditions regarding stability in biological media, using multidendate or macrocyclic approaches, and optimization of the linear and nonlinear photophysical properties *i.e.* the 1P- and/or 2P-brightness ($B^{(1)} = \varepsilon \cdot \phi$ and $B^{(2)} = \sigma \cdot \phi$) where ε , σ and ϕ represent the molecular 1P-extinction coefficient, 2P-cross-section and luminescence quantum yield, respectively. This latter point necessitates to avoid the presence of water molecules in the first coordination sphere and to adapt the nature of the antenna ligand. During this last decade a large variety of complexes has been reported by several authors such as Wong, Parker, Raymond, Bünzli, Petoud, Zhang and Charbonnière and collaborators.^[4] A valuable strategy to optimize the brightness consists in taking advantage of charge transfer (CT) antennas to increase simultaneously 1P- and 2P-absorption coefficients and displace the excitation wavelengths to the visible due to a direct sensitization mechanism.^[5] In this context, following our initial report in 2008 on functionalized CT-antennas tris-dipicolinate europium complexes,^[6] we systematically explored the effect of such functionalization using existing polydentate^[7a,b] or macrocyclic complexes such as cyclen^[7a] bis-bipyridine,^[7c] tacn,^[7d,e] pycen^[7f] and diMe-cyclen^[3c,7g] ($[\text{LnL}^{1a-c}]^+$, Figure 1). It appears that anionic polydentate and neutral tacn and pycen complexes featuring CT antennas are among the brightest complexes reported in the literature for Eu^{3+} and/or Tb^{3+} , but are not able to stain living cells through passive internalization processes.^[7b,d,e,f] On the other hand, cationic bis-pyridine or diMe-cyclen ($[\text{LnL}^{1b,c}]^+$, Figure 1) complexes exhibit lower quantum yield efficiency due to partial coordination of a water molecule and/or increased fluxionality in protic solvents but showed spontaneous internalization in living cells.^[7c,g] A similar charge effect was already described by Parker and Bünzli, who proposed a passive non-diffusive internalization process based on macropinocytosis with a localisation of the complexes in endosomal vesicles inside the cytosol.^[8]

In this study, we pursue this strategy by using a cross-bridged cyclam macrocycle (cb-cyclam) decorated with two pendant picolinate moieties, described by some of us to give extremely stable and inert lanthanide complexes ($[\text{LnL}^{2a}]^+$, Figure 1), that also present luminescent properties.^[9] While lanthanide(III) complexes based on a simple functionalized cyclam framework are typically unstable due to the unadapted size of the aza-ring, the cross-bridged (cb) constrained ligand (based on cb-cyclam 1, scheme 1, attached to picolinate arms), yielded exceptionally and unprecedented inert chelates. This unprecedented stability with Ln^{3+} ions relies on a *cis-V geometry*, leading to a very strong interaction between the macrocyclic nitrogen donor atoms of the macrocycle and the metal ion.^[9] In an effort to add value to this original compound, we turned to the synthetic and photophysical challenge raised by the improvement of the optical properties of the corresponding Eu and Yb complexes.

We report here the synthesis and chemical characterization of cb-cyclam ligands functionalized, via their pyridinic moiety, by donor- π -conjugated antennas (alkoxyphenylethynyl L^{2b} and dialkylaminephenylethynyl L^{2c}) and their corresponding europium(III) and ytterbium(III) complexes (Figure 1). The photophysical properties have been thoroughly studied and the



Scheme 1. Synthesis of the $[\text{LnL}^{2b-c}]^+$ complexes starting from cross-bridged cyclam 1. EDG stand for Electron Donating Group.

results are compared to those obtained with our first generation of complexes, and especially the diMe-cyclen based complexes (Figure 1), to emphasize the improvements provided by the constrained structure in addition to its previously demonstrated inertness. Finally, these compounds spontaneously internalize into living cells that can be imaged by two-photon microscopy.

Results and Discussion

Synthesis. As presented on Scheme 1, the synthesis started with the N^1, N^6 -dialkylation of cross-bridged cyclam 1^[10] with the corresponding mesylated picolinate antennas 2^b ^[7a,c] or 2^c ^[3a] in basic medium (K_2CO_3) and in the presence of NaI to accelerate the reaction rate. The diesters 3^b and 3^c were characterized by ^1H and ^{13}C NMR and HR-MS analysis before being placed in a biphasic mixture of $\text{KOH}_{(aq)}$ 6M/THF for 3^b and $\text{NaOH}_{(aq)}$ 4M/THF for 3^c to hydrolyze the ester functions. L^{2b} and L^{2c} were obtained as potassium carboxylate salts that were used without further purification. The complexation of dipicolinate cross-bridged cyclam derivatives with Ln^{3+} ions requires the use of solvents with high boiling point.^[9] The reaction was then performed in *n*-butanol (T_{eb} 117.7°C) with di-isopropylethylamine (DIPEA) as basic agent. The formation of the Ln^{3+} chelates is also very slow and needs long reaction times, but those could however be reduced by using microwave radiations as it was demonstrated with Yb^{3+} (8h by microwave compared to 5 days refluxing with Eu^{3+}). These harsh conditions can explain the formation of many side products and

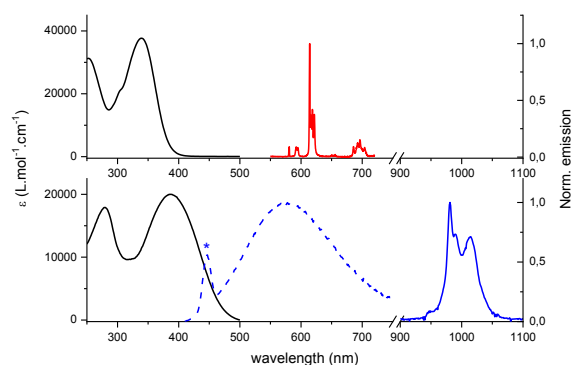


Figure 2. Absorption and emission spectra of the CT-functionalized complexes $[\text{EuL}^{2b}]^+$ ($\lambda_{\text{ex}} = 350$ nm, top) and $[\text{YbL}^{2c}]^+$ ($\lambda_{\text{ex}} = 387$ nm bottom) in water at room temperature, ($c \approx 10^{-5}$ Mol.L $^{-1}$ for absorption and 10^{-6} Mol.L $^{-1}$ for emission; * indicate Raman scattering signal).

Table 1. Photophysical data of europium and ytterbium complexes in various solvents at room temperature.

| | | λ_{max} (nm) | ϵ (L.mol $^{-1}$.cm $^{-1}$) | Φ ^[a] | τ (μs) | q |
|-----------------------|----------|--------------------------------|--|-----------------------|-----------------------------|-----|
| $[\text{EuL}^{2b}]^+$ | H $_2$ O | 339 | 38000 | 0.06 | 550 | 0.2 |
| | D $_2$ O | | | 0.11 | 770 | |
| | MeOH | 343 | 52000 | 0.25 | 740 | |
| | DMSO | 340 | | 0.45 | 900 | |
| $[\text{YbL}^{2c}]^+$ | H $_2$ O | 387 | 20000 | | 3.3 | 0.1 |
| | D $_2$ O | | | | 5.3 | |
| | MeOH | 401 | 32000 | | 3.5 | |
| | DCM | 405 | 28000 | | 4.8 | |

The relative error for ϵ and ϕ is +/- 5%.

^[a] Using quinine bisulfate in H $_2$ SO $_4$ 0.5M as standard ($\Phi = 0.546$) and an excitation wavelength of 338 nm in H $_2$ O and MeOH and 340 nm for DMSO..

consequently the low yields (~25 %), comparable to those of the $[\text{LnL}^{2a}]^+$ (Ln = Eu, Tb) compounds.^[9] After purification by semi-preparative HPLC, the purity of the final $[\text{LnL}^{2b-2c}]^+$ complexes was confirmed by analytical HPLC and HR-MS analysis (see Figures S1-S6 in Supporting Information).

Photophysical properties. Thanks to the amphiphilic nature of the polyethylene glycol moieties — here a tri-ethyleneglycol, (CH $_2$ CH $_2$ O) $_3$ CH $_3$ — the complexes are soluble both in water and in organic solvents (dichloromethane, methanol, DMSO), enabling the study of their photophysical properties in this large variety of media (Table 1). The room temperature absorption and emission spectra are reported in water (Figure 2). As usually observed, the absorption is dominated by the nature of the donor- π -conjugated picolinate antennas inducing a strongly allowed charge-transfer transition (CT) shifted in the visible compared to the non-functionalized parent complex $[\text{EuL}^{2a}]^+$ ($\lambda_{\text{max}} = 274$ nm in water, Figure 2). Quantitatively, the introduction of an alkoxyphenylethynyl chromophore resulted in a maximal

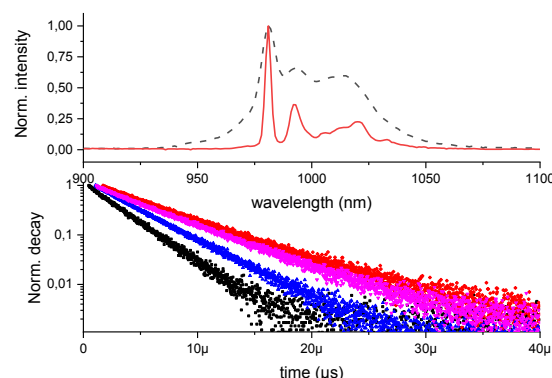


Figure 3. NIR emission spectra for $[\text{YbL}^{2c}]^+$ in MeOH/EtOH, 1:4 v/v) at room temperature (dashed black line) and 77K (solid red line) under 400 nm excitation (top) and lifetime decay recorded in water (black), MeOH (blue), DCM (magenta) and D $_2$ O (red) at room temperature under 980 nm excitation (bottom).

absorption at 339 nm in water with a cut-off close to 400 nm ($\Delta\lambda_{\text{max}} = 65$ nm compared to $[\text{EuL}^{2a}]^+$). When installing a stronger dialkylamino donor, an even more pronounced red shift with $\lambda_{\text{max}} = 387$ nm ($\lambda_{\text{cut-off}} = 480$ nm, $\Delta\lambda_{\text{max}} = 113$ nm) was observed. Consequently, the introduction of such CT-antennas enables the use of excitation source above 330 nm such as the N $_2$ laser (337 nm) or the cheaper 405 nm blue LED and basic glass sample holder and microscopy optics. Upon excitation in this CT-absorption band, the characteristic Eu $^{3+}$ and Yb $^{3+}$ emission profiles were detected (Figure 2). In the case of $[\text{EuL}^{2b}]^+$, the luminescence pattern was assigned to $^5\text{D}_0 \rightarrow ^7\text{F}_J$ ($J = 0$ to 4) transitions without any remaining ligand-centred emission, the signature of an efficient sensitization process. $[\text{YbL}^{2c}]^+$, however, displayed a dual emission consisting of a broad CT band in the visible ($\lambda_{\text{em}} = 554$ nm) that is due to a residual ligand-centred emission — indicative of an incomplete energy transfer to the metal, accompanied by the NIR signature of Yb(III) assigned to $^2\text{F}_{5/2} \rightarrow ^2\text{F}_{7/2}$ (980-1040 nm).

Quantum yields and lifetimes were measured in protic and aprotic solvents including deuterated water (Table 1) allowing us to determine the hydration number “q” using the phenomenological equation of Beeby *et al.*^[11] A value of 0.2 was obtained for $[\text{EuL}^{2b}]^+$ similar to that of the parent complex ($q = 0.25$ -0.35 for $[\text{EuL}^{2a}]^+$)^[9a] and 0.1 for $[\text{YbL}^{2c}]^+$. Interestingly, these values are lower than that of their diMe-cyclen analogues (0.5 and 0.2 for $[\text{EuL}^{1b}]^+$ and $[\text{YbL}^{1c}]^+$, respectively)^[7g,3c] suggesting that the more sterically constrained cross-bridged cyclam scaffold offers a stronger protection against water coordination (*vide infra*). This conclusion is further corroborated by longer lifetimes observed in water for the cb-cyclam based complexes compared to their diMe-cyclen analogues and the six-fold increase of the quantum yield measured for $[\text{EuL}^{2b}]^+$ (0.06 vs 0.01 for $[\text{EuL}^{1b}]^+$)^[7g]. The lifetime of 3.3 μs in water of the complex $[\text{YbL}^{2c}]^+$ makes it comparable to the best Yb $^{3+}$ emitters^[3a,12] among the non-deuterated or non-fluorinated complexes.^[13] This value remains of course much lower than that of the exceptional Yb $^{3+}$ perfluorinated porphyrinate

ARTICLE

Table 2. Photophysical data of europium(III) complex [EuL^{2b}]⁺ in different solvents at room temperature.

| | Φ | τ (ms) | τ_r (ms) | η_{Eu} | η_{sens} | $I_{J=1}/I_{tot}$ | k_r (s ⁻¹) | Σk_{nr} (s ⁻¹) |
|------------------|--------|----------------|------------------|-------------|---------------|-------------------|-----------------------------|---------------------------------------|
| H ₂ O | 0.06 | 0.55 | 1.70 | 0.32 | 0.19 | 0.059 | 588 | 1230 |
| D ₂ O | 0.11 | 0.77 | 1.92 | 0.40 | 0.28 | 0.066 | 520 | 779 |
| MeOH | 0.25 | 0.74 | 1.86 | 0.40 | 0.63 | 0.064 | 537 | 814 |
| DMSO | 0.45 | 0.90 | 1.79 | 0.50 | 0.90 | 0.085 | 558 | 553 |

τ_r is the radiative lifetime, $k_r = 1/\tau_r = A(0,1) \cdot n^3 [I_{tot}/I_{J=1}]$ where $A(0,1)$ is the spontaneous emission probability in vacuum determined to 14.65 s⁻¹ and n is the refractive index of the solvent. $\Sigma k_{nr} = 1/\tau - 1/\tau_r$

complex recently reported by Zhang and co-workers that enabled whole mice body imaging.^[14]

In contrast, the luminescence quantum yield in water of the europium(III) complex and consequently its brightness ($B^{(1)} = 2280 \text{ L}\cdot\text{mol}^{-1}\cdot\text{cm}^{-1}$ at 340 nm) remain modest and far lower than the record values obtained for tacn, pyclen, polydentate complexes ($B^{(1)}$ in the range of 15000-20000 $\text{L}\cdot\text{mol}^{-1}\cdot\text{cm}^{-1}$).^[7] Remarkably, in aprotic solvents like DMSO the quantum yield is far higher (0.45) and consequently the brightness becomes comparable to the above mentioned values. In order to get deeper insight into this strong solvent effect, the relevant radiative and non-radiative constants were determined using the method proposed by Beeby *et al.* and Werts *et al.* (Table 2).^[15] In all solvents the radiative lifetime, the ratio between the magnetic dipole transition ($J=1$) and the total emission intensity (I_{tot}) are almost constant indicating that the complex conserved the same symmetry in all media, and consequently the radiative lifetime (τ_r) and the radiative constant (k_r) are similar. In marked contrast the decrease of the lifetime from DMSO to methanol and water results in a significant increase of the non-radiative constant from 553 to 1230 s⁻¹. These observations explain the decrease of the quantum yield in protic solvents and strongly suggest an additional quenching mechanism due to the presence of O-H vibrators in the vicinity of the europium emitters. Since a q value of 0.2 was measured, only a partial coordination to the Eu³⁺ ion can be envisaged or an indirect quenching mechanism mediated by hydrogen bonding *via* the carbonyl moieties of the picolinate chelators.

Structure of the complexes in solution. Since both Yb(III) and Eu(III) emission spectra are highly sensitive to the overall symmetry of the first coordination sphere, the symmetry of the complexes [EuL^{2b}]⁺ and [YbL^{2c}]⁺ in solution was investigated thanks to their low temperature emission spectra recorded in MeOH/EtOH organic glass at optimal resolution (Figures 3, 4). In the case of [YbL^{2c}]⁺, decreasing the temperature reduced the inhomogeneous line broadening but the resolution of the 77K spectrum was not high enough to get a clear picture of the ligand field splitting (*LFS*) of the ²F_{7/2} ground state (expected *LFS* in 4 transitions). However the maximal *LFS* can be estimated to 513 cm⁻¹ (Figure 3), an intermediate value between *D*₃ (340-370 cm⁻¹)^[16] and *C*_{2v} complexes like the diMe-cyclen analogues [YbL^c]⁺

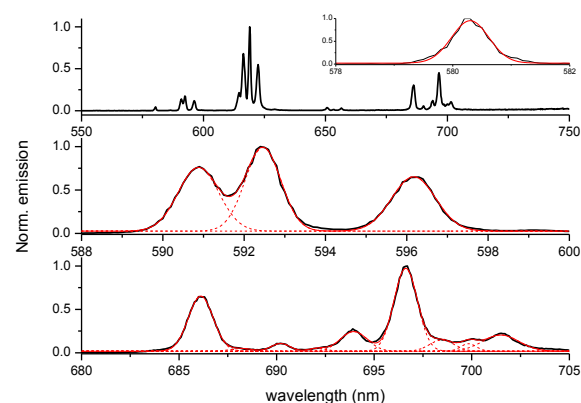


Figure 4. 77K emission spectra of [EuL^{2b}]⁺ (black) in organic glass (MeOH/EtOH, 1:4 v/v) under 345 nm excitation with optimal resolution (detection slit 0.2, increment 0.2 nm). (Top) Full spectra, in inset is represented the magnification of the J=0 transition emission spectrum with a single Gaussian deconvolution (red). (Middle) Magnification of the J=1 transition and decomposition in three Gaussian curves (dashed red, sum in red). (Bottom) Magnification of the J=4 transition and decomposition in nine Gaussian curves (dashed red, sum in red).

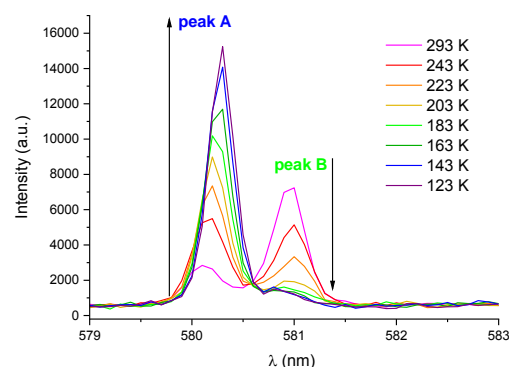


Figure 5. Evolution of the J=0 emission bands with temperature recorded for [EuL^{2b}]⁺ in MeOH/EtOH, 1:4 v/v) under 345 nm excitation with optimal resolution.

($LFS^{\max}=670 \text{ cm}^{-1}$).^[3c] In the case of [EuL^{2b}]⁺ the low temperature emission spectrum (Figure 4) is better resolved: the ⁵D₀→⁷F₀ transition, insensitive to any *LFS* effect, presents a mono-Gaussian shape characteristic of a single emissive species at 77K. Although the $J = 2$ transition can be decomposed into 4 overlapping sub-components, both $J = 1$ and $J = 4$ transitions present a multiplicity of 3 and 9 respectively, and the presence of 2J+1 sub-components is a clear signature of a low symmetry complex.^[17] For this compound, the relative intensities of the ⁵D₀→⁷F_J ($J = 0$ to 4) transitions is the following 0.1, 1, 8.3, 0.2, 3.3 using the $J = 1$ transition as internal standard. This distribution results in a concentration $R^2 = 64.2\%$ of the total intensity in the hypersensitive $J = 2$ band and an r value of 2.5, r being defined as the ratio between the intensity of the $J = 2$ over $J = 4$ transition. These two parameters are qualitative indicators of the symmetry of the coordination polyhedron. Comparison with similar parameters in

ARTICLE

other macrocyclic complexes featuring similar antennas confirmed that they are lower than that of the C_3 symmetric tacn based complex ($r = 10.9$, $R^2 = 79\%$) but compare well with those of C_2 diMe-cyclen [EuL^{1b}] $^+$ ($r = 2.5$, $R^2 = 56\%$)^[79] and distorted C_3 pycnen derivatives ($r = 3.0$, $R^2 = 65\%$).^[77] Contrarily to what we observed at 77K, at room temperature the $J = 0$ transition of [EuL^{2b}] $^+$ presents two components at 581 (main peak B, Figure 5) and 580.1 nm (minor peak A, Figure 5) signature of the presence of at least two different emitting species. A step-by-step temperature variation indicated that these two species are interconverting and tend towards a single species at low temperature (peak A) (Figure 5). The expected isobestic point for such equilibrium was not clearly observed due to the inherent line shifts resulting from the variation of temperature.^[18] In other words, this solution study indicated that these complexes present a symmetry intermediate between that of pycnen and diMe-cyclen picolinate derivatives with the presence of two isomers in interconversion. Due to the C_2 symmetry of the cyclam scaffold, two isomers can be formed depending on the relative configuration of the picolinate arms along the C_2 axis. The geometry of these two isomers noted A and B, was investigated using density functional theory (DFT, see computational details in Experimental Section) on yttrium models [YL^{2b}] $^+$ where the peg end groups were replaced with methyl fragments. Both optimized

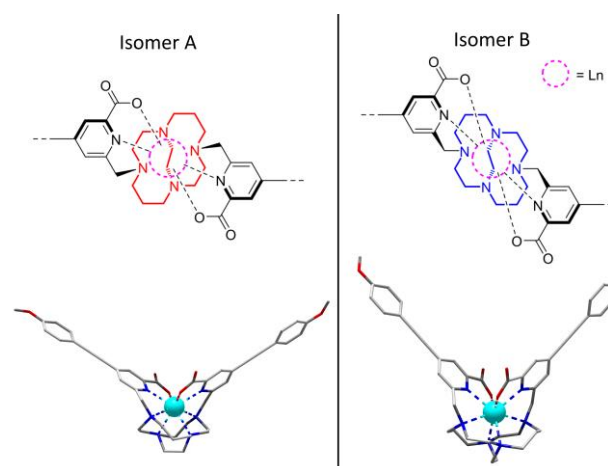


Figure 6. DFT optimized geometry of the two possible conformations of the model complex [YL^{2b}] $^+$.

structures are given in Figure 6. Isomer B is only 12.7 kcal.mol $^{-1}$ less stable than Isomer A, potentially explaining its observation at room temperature and complete preference for Isomer A at lower temperature. Furthermore, the eventual partial water coordination

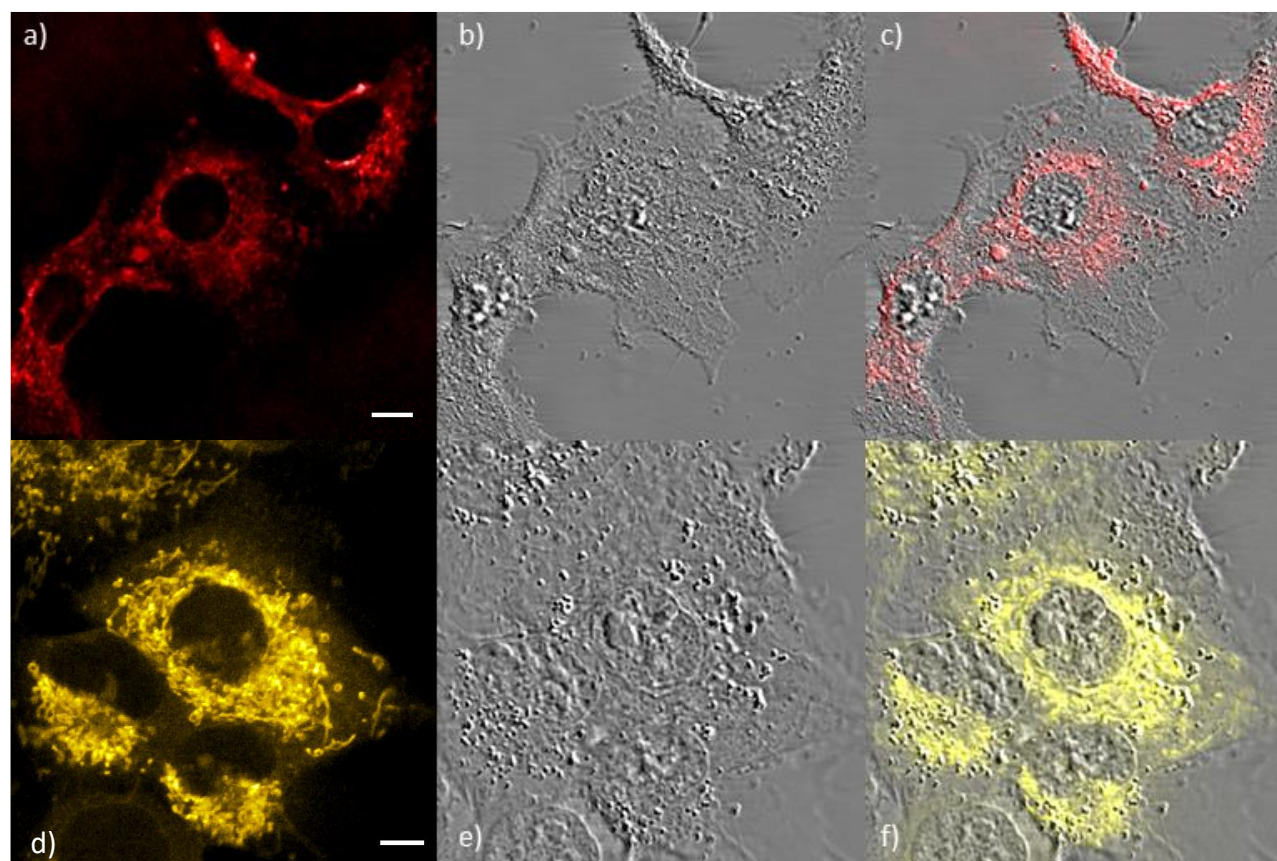


Figure 7. 2P imaging of living T24-cells stained with [EuL^{2b}] $^+$, $\lambda_{\text{ex}} = 780$ nm (a), and [YbL^{2c}] $^+$, $\lambda_{\text{ex}} = 800$ nm (d) using conventional microscope, corresponding transmitted light DIC images (b, e) and merging of the DIC and biphotonic images (c, f). Complexes were added in the cell medium in phosphate buffer solution to reach a final concentration of $5 \cdot 10^{-6}$ mol.L $^{-1}$. Scale bars 10 μm .

ARTICLE

was theoretically investigated on these two isomers using diamagnetic rare-earths featuring different ionic radius namely La^{3+} , Y^{3+} and Lu^{3+} . Stable adducts have been obtained only in the case of Isomer A with the larger size $\text{La}^{3+}/\text{Y}^{3+}$ ions (Figure S7). In all other cases, the water molecule was systematically expelled from the coordination sphere (isomers B and Lu isomer A). This result is in perfect agreement with the almost zero hydration number observed for the Yb^{3+} complex featuring an ionic radius close to that of Lu^{3+} (both isomers expel the water molecules). In contrast, in the case of the Eu^{3+} complex whose ionic radius is intermediate between La^{3+} and Y^{3+} , partial water coordination should be possible for Isomer A explaining the $q=0.2$ hydration number value and the modest luminescence quantum yield.

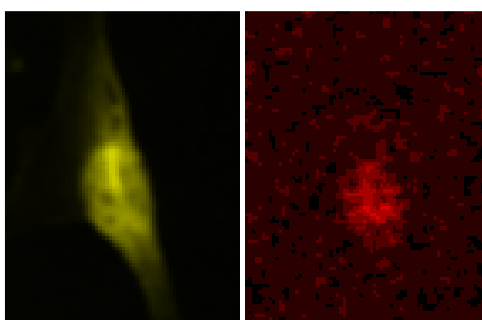


Figure 8. 2P imaging fixed HeLa-cells stained with $[\text{YbL}^{2c}]^+$ in the NIR-to-vis configuration and in the NIR-to-NIR configuration. Complexes were added in the cell medium in phosphate buffer solution to reach a final concentration of $5\text{-}10 \times 10^{-6} \text{ mol.L}^{-1}$.

Two-photon microscopy imaging. The complexes $[\text{EuL}^{2b}]^+$ and $[\text{YbL}^{2c}]^+$ possess the same CT-antennas responsible for the two-photon absorption properties than their diMe-cyclen counterparts (same chromophores and same number) and can therefore be assumed to present similar 2PA cross-sections. These complexes were tested in 2P-bioimaging experiments using living T24 cells or fixed HeLa cells (staining concentration of $5\text{-}10 \times 10^{-6} \text{ mol.L}^{-1}$). First experiments were conducted on a conventional LSM710 NLO microscope (Carl Zeiss) with living T24 cells after 4h of incubation followed by rinsing. Excitation was performed in the NIR at 780 and 800 nm for $[\text{EuL}^{2b}]^+$ and $[\text{YbL}^{2c}]^+$ respectively and detection was performed at higher energy compared to the excitation, in the red (Eu^{3+} emission or residual CT emission for the Yb^{3+} complex). In the case of Eu-LLB, the quality of the images was excellent with a high contrast and high signal-to-noise (Figures 7). In the case of living cells imaging (Figure 7), the images clearly indicate that the complexes were spontaneously internalized and localized in the perinuclear area of the cytosol. It is also possible to discriminate the circular and filamentous organelles, accumulating the dyes, that may correspond to endocytic vesicles and mitochondria as previously observed by co-localization experiments in the case of diMe-cyclen analogues.^[3c,7g] As previously reported for cationic LLBs, the presence of such stained vesicles indicates that the passive internalisation mechanism occurs *via* endocytosis or pinocytosis. The labelling of the living polarized mitochondria is a common feature of the cationic dyes, such as Rhodamine 123, TMRE or MitoTracker® due to the negative mitochondrial membrane

potential generated by proton pumps. This strong accumulation suggests an additional mechanism of the passive transmembrane diffusion of LLB.

Conclusion

We reported here the synthesis and chemical characterization of cb-cyclam dipicolinate ligands functionalized by donor- π -conjugated antennas (alkoxyphenylethynyl and dialkylaminephenylethynyl) and their corresponding europium(III) and ytterbium(III) complexes. The photophysical properties have been thoroughly studied and reveal (i) an increased brightness for the Eu^{3+} complex with still a pronounced sensitivity to protic solvents, (ii) the excellent photophysical properties of the Yb^{3+} analogue despite (iii) the presence of two isomers in equilibrium. Results were compared to those obtained with our first generations of complexes to emphasize the improvements provided by the constrained structure in addition to its previously demonstrated inertness. Finally, these compounds spontaneously internalized into living cells that were imaged by two-photon microscopy.

Experimental Section

Photophysical measurements in solution. Absorption spectra were recorded on a JASCO V-650 spectrophotometer as solutions in spectrophotometric-grade methanol or water (ca. 10^{-5} or $10^{-6} \text{ mol.L}^{-1}$). Emission spectra were measured using a Horiba-Jobin-Yvon Fluorolog-3 fluorimeter. Spectra were corrected for both excitation-source light-intensity variation and emission spectral responses. Luminescence lifetimes were obtained by pulsed excitation with a FL-1040 UP xenon lamp. Luminescence quantum yields, Φ , were measured with diluted solutions in water or organic solvents with an absorbance of less than 0.1 by using equation (1):

$$\frac{\Phi_x}{\Phi_r} = \frac{A_r(\lambda)}{A_x(\lambda)} \frac{n_x^2}{n_r^2} \frac{D_x}{D_r} \quad (1)$$

in which A is the absorbance at the excitation wavelength (λ), n is the refractive index, and D is the integrated luminescence intensity; r and x stand for reference and sample, respectively. The reference is quinine bisulfate in a 1N aqueous solution of sulfuric acid ($\Phi_r = 0.546$). Excitation of reference and sample compounds was performed at the same wavelength. Practically, for each sample, series of measurements are performed with different absorbance ranging from 0.1 to 0.01. The plot of the integrated luminescence intensity vs. absorbance gives straight line with excellent correlation coefficients and the slope S can be determined. Equation (1) becomes (2):

$$\frac{\Phi_x}{\Phi_r} = \frac{S_x(\lambda)}{S_r(\lambda)} \frac{n_x^2}{n_r^2} \quad (2)$$

Live cell culture and treatment. T24 human epithelial bladder cancer cell line (ATCC no. HBT-4) was used. T24 cells were cultured in 25 cm^2 tissue-culture flasks (T25) at 37°C in a humidified atmosphere with 5% CO_2 . They were incubated in RPMI 1640 supplemented with 100 U mL^{-1} penicillin, 100 $\mu\text{g mL}^{-1}$ streptomycin, and 10% fetal calf serum (complete medium). Cells were grown to near confluence in the culture flasks and then suspended with a solution of 0.05% trypsin-ethylenediaminetetraacetic acid (EDTA; Sigma). Cells were placed on a LabTek I chambered cover glass (Nunc)

ARTICLE

at low cell density in complete culture medium 24 h before experiments. On the other hand, HeLa cells (Human cervical cancer cell ATCC CCL-2) were cultured in Dulbecco's modified Eagle's medium (DMEM) supplemented with 10% fetal bovine serum (Gibco ThermoFisher Scientific), in a humidified atmosphere containing 5% CO₂ at 37 °C. Cells were loaded at low density onto a glass coverslip in 24 wells plate (Corning) and cultured for 24 h before labelling. Cells were washed twice with PBS, fixed with 3% paraformaldehyde (Thermo Scientific Pierce) for 10 min, washed twice with PBS, and PFA is quenched with 50 mmol.L⁻¹ NH₄Cl for 10 min, washed twice with PBS, permeabilized with PBS-0.1% Triton X-100 for 10 min and washed two times with PBS. In both cases, the staining was performed by addition of a concentrated solution of complex (10⁻⁴ mol.L⁻¹) in PBS buffer to the cell culture medium to reach a final concentration of 5-10 × 10⁻⁶ mol.L⁻¹. The fixed cells are mounted with mounting medium (Southern Biotech).

Confocal and two-photon microscopy. The NIR-to-VIS two-photon experiments were performed using a LSM710 NLO (Carl Zeiss) confocal laser scanning microscope based on the inverted motorized stand (AxioObserver, Zeiss) in descanned detection mode with the open pinhole. The 2P excitation was provided by Ti:Sa femtosecond tuneable laser (Chameleon, Ultra II, Coherent). The [EuL^{2b}]⁺ complex was excited at 760 nm and detected using the PMT from 460 to 641 nm; the [YbL^{2b}]⁺ excited at 720 nm and detected using APD from 470 to 610 nm.

Computational details. DFT geometry optimizations were carried out with the Gaussian 09 (Revision D.01)^[19] package employing the PBE0 hybrid functional^[20] and tightening self-consistent field convergence thresholds (10⁻¹⁰ a.u.) and geometry optimization (10⁻⁵ a.u.) convergence thresholds. The "Stuttgart/Dresden" basis sets and effective core potentials were used to describe the yttrium atom,^[21] whereas all other atoms were described with the SVP basis sets.^[22] Solvent effects (solvent = water) were included through the Polarizable Continuum Model (PCM).^[23]

Acknowledgements

The authors are grateful to the referees for careful reading of the paper and valuable suggestions and comments. The authors also acknowledge support of the Ministère de l'Enseignement Supérieur et de la Recherche, the Centre National de la Recherche Scientifique, the Institut National de la Santé et de la Recherche Médicale and the Agence Nationale de la Recherche (SADAM ANR-16-CE07-0015-02). M.B. and R.T. thanks the "Service Commun de RMN" of the University of Brest. Confocal and 2P facility of the IAB platform was co-funded thanks to grants of "Association pour la Recherche sur le Cancer" (ARC, Villejuif, France), "Ligue vs Cancer" (LCC Isère/Ardèche) and the CPER program. B.L.G. thanks the French GENCI-CINES center for high-performance computing resources.

Conflict of interest: The authors declare no conflict of interest.

Keywords: Europium(III) • Ytterbium(III) • Luminescence • Bioprobe • Two-photon microscopy • Bioimaging

References

- [1] a) C. Andraud, O. Maury, *Eur. J. Inorg. Chem.*, **2009**, 4357-4371; b) Y. Ma, Y. Wang, *Coord. Chem. Rev.*, **2010**, *254*, 972-990; c) A. D'Aléo, C. Andraud, O. Maury, *Luminescence of Lanthanide Ions in Coordination Compounds and Nanomaterials* Ed. A. De Bettencourt-Diaz, Wiley **2014**, pp. 197-226;
- [2] a) H. Wang, X. Mu, J. Yang, Y. Liang, X.-D. Zhang, D. Ming, *Coord. Chem. Rev.* **2019**, *380*, 550-571; b) G. Hong, A. L. Antaris, H. Dai, *Nat Biomed Eng* **2017**, *1*, 0010; c) S. A. Hilderbrand, R. Weissleder, *Curr. Op. Chem. Biol.* **2010**, *14*, 71-79.
- [3] a) A. D'Aléo, A. Bourdolle, S. Bulstein, T. Fauquier, A. Grichine, A. Duperray, P. L. Baldeck, C. Andraud, S. Brasselet, O. Maury *Angew. Chem. Int. Ed.* **2012**, *51*, 6622-6625; b) A. T. Bui, A. Grichine, S. Brasselet, A. Duperray, C. Andraud, O. Maury *Chem. Eur. J.* **2015**, *21*, 17757-17761; c) A. T. Bui, M. Beyler, A. Grichine, A. Duperray, J.-C. Mulatier, C. Andraud, R. Tripier, S. Brasselet, O. Maury *Chem. Commun.* **2017**, *53*, 6005-6008.
- [4] a) C. P. Montgomery, B. S. Murray, E. J. New, R. Pal, D. Parker, *Acc. Chem. Res.* **2009**, *42*, 925-937; b) E. G. Moore, A. P. S. Samuel, K. N. Raymond, *Acc. Chem. Res.* **2009**, *42*, 542-552; c) J.-C. Bünzli, *Coord. Chem. Rev.* **2015**, *293-294*, 19-47; d) M. Sy, A. Nonat, N. Hildebrandt, L. J. Charbonnière *Chem. Commun.*, **2016**, *52*, 5080-5095; e) G.-L. Law, K.-L. Wong, C. W.-Y. Man, W.-T. Wong, S.-W. Tsao, M. H.-W. Lam, P. K.-S. Lam, *J. Am. Chem. Soc.*, **2008**, *130*, 3714-3715; f) J.-Y. Hu, Y. Ning, Y.-S. Meng, J. Zhang, Z.-Y. Wu, S. Gao, J.-L. Zhang, *Chem. Sci.* **2017**, *8*, 2702-2709; g) I. Martinic, S. V. Eliseeva, T. N. Nguyen, V. L. Pecoraro, S. Petoud *J. Am. Chem. Soc.*, **2017**, *139*, 8388-8391.
- [5] A. D'Aléo, L. Ouahab, C. Andraud, F. Pointillart, O. Maury, *Coord. Chem Rev.* **2012**, *256*, 1604-1620.
- [6] A. D'Aléo, A. Picot, A. Beeby, J.A. G. Williams, B. Le Guennic, C. Andraud, O. Maury, *Inorg. Chem.*, **2008**, *47*, 10258-10268.
- [7] a) A. D'Aléo, M. Allali, A. Picot, P. L. Baldeck, L. Toupet, C. Andraud, O. Maury *C. R. Chimie* **2010**, *13*, 681-690; b) H. Sund, Y.-Y. Liao, C. Andraud, A. Duperray, A. Grichine, B. Le Guennic, F. Riobé, H. Takalo, O. Maury *ChemPhysChem* **2018**, *19*, 3318-3324; c) A. Bourdolle, M. Allali, J.-C. Mulatier, B. Le Guennic, J. Zwier, P. L. Baldeck, J.-C.G. Bünzli, C. Andraud, L. Lamarque, O. Maury *Inorg. Chem.* **2011**, *50*, 4987-4999; d) M. Soulié, F. Latzko, E. Bourrier, V. Placide, S. J. Butler, R. Pal, J. W. Walton, P. L. Baldeck, B. Le Guennic, C. Andraud, J. M. Zwier, L. Lamarque, D. Parker, O. Maury *Chem. Eur. J.* **2014**, *20*, 8636-8646; e) A. T. Bui, A. Roux, A. Grichine, A. Duperray, C. Andraud, O. Maury *Chem. Eur. J.* **2018**, *24*, 3408-3412; f) N. Hamon, M. Galland, M. Le Fur, A. Roux, A. Duperray, A. Grichine, C. Andraud, B. Le Guennic, M. Beyler, O. Maury, R. Tripier *Chem. Commun.* **2018**, *54*, 6173-6176; g) A. T. Bui, M. Beyler, Y.-Y. Liao, A. Grichine, A. Duperray, J.-C. Mulatier, B. Le Guennic, C. Andraud, O. Maury and R. Tripier, *Inorg. Chem.*, **2016**, *55*, 7020-7025.
- [8] a) E. J. New, D. Parker, D. G. Smith, J. W. Walton, *Curr. Op. Chem. Biol.* **2010**, *14*, 238-246; b) S. J. Butler, B.K. McMahon, R. Pal, D. Parker, J. W. Walton, *Chem. Eur. J.* **2013**, *19*, 9511-9517; c) E. Deiters, B. Song, A.-S. Chauvin, C. D. B. Vandevyver, F. Gumy J.-C. G. Bünzli, *Chem. Eur. J.*, **2009**, *15*, 885-900.
- [9] a) A. Rodriguez-Rodriguez, D. Esteban-Gomez, R. Tripier, G. Tircso, Z. Garda, I. Toth, A. de Blas, T. Rodriguez-Blas, C. Platas-Iglesias, *J. Am. Chem. Soc.* **2014**, *136*, 17954-17957; b) A. Rodriguez-Rodriguez, M. Regueiro-Figueroa, D. Esteban-Gomez, R. Tripier, G. Tircso, K. Kalman, Ferenc; C. A. Benyei, I. Toth, A. de Blas, T. Rodriguez-Blas, C. Platas-Iglesias *Inorg. Chem.* **2016**, *55*, 2227-2239.
- [10] E. H. Wong, G. R. Weisman, D. C. Hill, D. P. Reed, M. E. Rogers, J. S. Condon, M. A. Fagan, J. C. Calabrese, K.-C. Lam, I. A. Guzei, A. L. Rheingold, *J. Am. Chem. Soc.* **2000**, *122*, 10561-10572.
- [11] A. Beeby, I. M. Clarkson, R. S. Dickens, S. Faulkner, D. Parker, L. Royle, A. de Sousa, J. A. G. Williams and M. Woods, *J. Chem. Soc., Perkin Trans. 2*, **1999**, 493-504.
- [12] a) E. G. Moore, J. Xu, S. C. Dodoni, C. J. Jocher, A. D'Aléo, M. Seitz, K. Raymond, *Inorg. Chem.* **2010**, *49*, 4156-4166; b) S. Comby, D. Imbert, C. Vandevyver, J.-C. G. Bünzli, *Chem. Eur. J.* **2007**, *13*, 936-944; c) M. H. V. Werts, R. H. Woudenberg, P. G. Emmerink, R. van Gassel, J. W. Hofstraat; J. W. Verhoeven, *Angew. Chem. Int. Ed.* **2000**, *39*, 4542-4544.
- [13] a) C. Doffek, M. Seitz, *Angew. Chem. Int. Ed.* **2015**, *54*, 9719-9721; b) J.-Y. Hu, Y. Ning, Y.-S. Meng, J. Zhang, Z.-Y. Wu, S. Gao, J.-L. Zhang,

ARTICLE

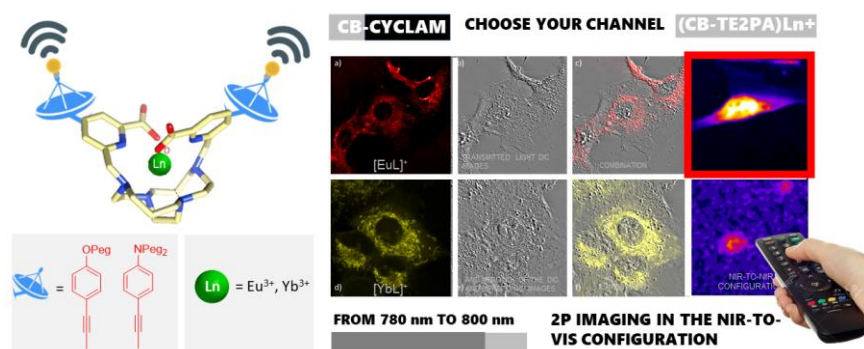
- Chem. Sci.* **2017**, *8*, 2702-2709; c) N. Sourı, P. Tian, C. Platas-Iglesias, K.-L. Wong, A. Nonat, L. J. Charbonniere, *J. Am. Chem. Soc.* **2017**, *139*, 1456-1459; d) Y. Ning, J. Tang, Y.-W. Liu, J. Jing, Y. Sun, J.-L. Zhang *Chem. Sci.* **2018**, *9*, 3742-3753.
- [14] Y. Ning, S. Chen, H. Chen, J.-X. Wang, S. He, Y.-W. Liu, Z. Cheng, J.-L. Zhang *Inorg. Chem. Front.* **2020** DOI: 10.1039/C9QI01132C.
- [15] a) M. H. V. Werts, R. T. F. Jukes, J. W. Verhoeven, *Phys. Chem. Chem. Phys.* **2002**, *4*, 1542-1548; b) A. Beeby, L. M. Bushby, D. Maffeo, J. A. G. Williams, *J. Chem. Soc., Dalton Trans.* **2002**, 48-54.
- [16] a) . Reinhard, H. U. Gudel, *Inorg. Chem.* **2002**, *41*, 1048-1055; b) F. Silva, O. L. Malta, C. Reinhard, H. U. Gudel, C. Piguat, J. E. Moser, J. C. G. Bunzli, *J. Phys. Chem. A* **2002**, *106*, 1670-1677; c) X. Yi, K. Bernot, V. Le Corre, G. Calvez, F. Pointillart, O. Cador, B. Le Guennic, J. Jung, O. Maury, V. Placide, Y. Guyot, T. Roisnel, C. Daiguebonne, O. Guillou, *Chem. Eur. J.* **2014**, *20*, 1569-1576.
- [17] a) S. V. Eliseeva, J.-C. G. Bünzli, in *Chap 1 Springer series on fluorescence, Vol. 7, Lanthanide spectroscopy, Materials, and Bio-applications, ed. P. Hännen and H. Härmä, Springer Verlag, Berlin, Vol. 7, 2010*; b) P. A. Tanner *Chem. Soc. Rev.* **2013**, *42*, 5090-5101; c) K. Biennemans *Coord. Chem. Rev.* **2015**, *295*, 1-45.
- [18] H. Kusama, O. J. Sovers, T. Yoshioka, *Jap. J. Appl. Phys.* **1976**, *15*, 2349-2358.
- [19] Gaussian 09, Revision D.01, M. J. Frisch, G. W. Trucks, H. B. Schlegel, G. E. Scuseria, M. A. Robb, J. R. Cheeseman, G. Scalmani, V. Barone, B. Mennucci, G. A. Petersson, H. Nakatsuji, M. Caricato, X. Li, H. P. Hratchian, A. F. Izmaylov, J. Bloino, G. Zheng, J. L., Sonnenberg, M. Hada, M. Ehara, K. Toyota, R. Fukuda, J. Hasegawa, M. Ishida, T. Nakajima, Y. Honda, O. Kitao, H. Nakai, T. Vreven, J. A. Montgomery, Jr., J. E. Peralta, F. Ogliaro, M. Bearpark, J. J. Heyd, E. Brothers, K. N. Kudin, V. N. Staroverov, T. Keith, R. Kobayashi, J. Normand, K. Raghavachari, A. Rendell, J. C. Burant, S. S. Iyengar, J. Tomasi, M. Cossi, N. Rega, J. M. Millam, M. Klene, J. E. Knox, J. B. Cross, V. Bakken, C. Adamo, J. Jaramillo, R. Gomperts, R. E. Stratmann, O. Yazyev, A. J. Austin, R. Cammi, C. Pomelli, J. W. Ochterski, R. L. Martin, K. Morokuma, V. G. Zakrzewski, G. A. Voth, P. Salvador, J. J. Dannenberg, S. Dapprich, A. D. Daniels, O. Farkas, J. B. Foresman, J. V. Ortiz, J. Cioslowski, D. J. Fox, Gaussian, Inc., Wallingford CT, 2013.
- [20] a) J. P. Perdew, K. Burke, M. Ernzerhof, *Phys. Rev. Lett.* **1996**, *77*, 3865-3868; b) C. Adamo, V. Barone, *J. Chem. Phys.* **1999**, *110*, 6158-6170.
- [21] M. Dolg, H. Stoll, H. Preuss, *Theor. Chim. Acta* **1993**, *85*, 441-450.
- [22] F. Weigend, R. Ahlrichs, *Phys. Chem. Chem. Phys.* **2005**, *7*, 3297-3305.
- [23] J. Tomasi, B. Mennucci, R. Cammi, *Chem. Rev.* **2005**, *105*, 2999-3093.

ARTICLE

Entry for the Table of Contents (Please choose one layout)

Layout 1:

ARTICLE



J. Mendy, A.-T. Bui, A. Roux, J.-C. Mulatier, D. Curton, A. Duperray, A. Grichine, Y. Guyot, S. Brasselet, F. Riobé, C. Andraud, B. Le Guennic, V. Patinec, R. Tripier, M. Beyler* and O. Maury**

Page No. – Page No.

Cationic Biphotonic Lanthanide Luminescent Bioprobes Based on Functionalized Cross-Bridge Cyclam Macrocycles.

Table of contents text: Cationic two-photon europium and ytterbium luminescent bioprobes based on cross-bridged cyclam macrocycle functionalized by charge transfer antenna showed spontaneous internalization in living cells.